

# Capacity and QoS for a Scalable Ring-Based Wireless Mesh Network

Jane-Hwa Huang, Li-Chun Wang, *Senior Member, IEEE*, and Chung-Ju Chang, *Fellow, IEEE*

**Abstract**—The wireless mesh network (WMN) is an economical solution to support ubiquitous broadband services. This paper investigates the tradeoffs among quality-of-service (QoS), capacity, and coverage in a scalable multichannel ring-based WMN. We suggest a simple frequency planning in the proposed ring-based WMN to improve the capacity with QoS support, and to make the system more scalable in terms of coverage. We develop a physical (PHY)/medium access control (MAC) cross-layer analytical model to evaluate the delay, jitter, and throughput of the proposed WMN, by taking account of the carrier sense multiple-access (CSMA) MAC protocol, and the impact of hop distance on transmission rate in the physical layer. Furthermore, the mixed-integer nonlinear programming optimization approach is applied to determine the optimal number of rings and the associated ring widths, aiming at maximizing the capacity and coverage of a mesh cell subject to the delay requirement.

**Index Terms**—Capacity and coverage, cross-layer analysis, quality-of-service (QoS), wireless mesh network (WMN).

## I. INTRODUCTION

THE WIRELESS MESH NETWORK (WMN) is a promising technology for next-generation wireless systems since it can enhance coverage with low transmit power [1]–[4]. The architecture for a WMN is illustrated in Fig. 1, where each user relays other users' traffic toward the central gateway directly connected to the Internet. Compared with single-hop networks, the coverage of WMN is improved thanks to less propagation loss and shadowing. Moreover, WMN can be rapidly deployed in a large-scale area with less cabling engineering work.

However, multihop networking may face the scalability issue [3]–[5]. Specifically, the multihop communications can extend the coverage of an access point with more hops or longer hop distance. However, the repeatedly relayed traffic with more hops will easily exhaust the radio resource and degrade the quality-of-service (QoS), e.g., longer delay and higher jitter. In the meanwhile, longer hop distance will also lead to lower data rate in the relay link between nodes. Besides, as the number of users increases, more collisions due to channel contention will further degrade the throughput. Therefore, one of the key challenges in

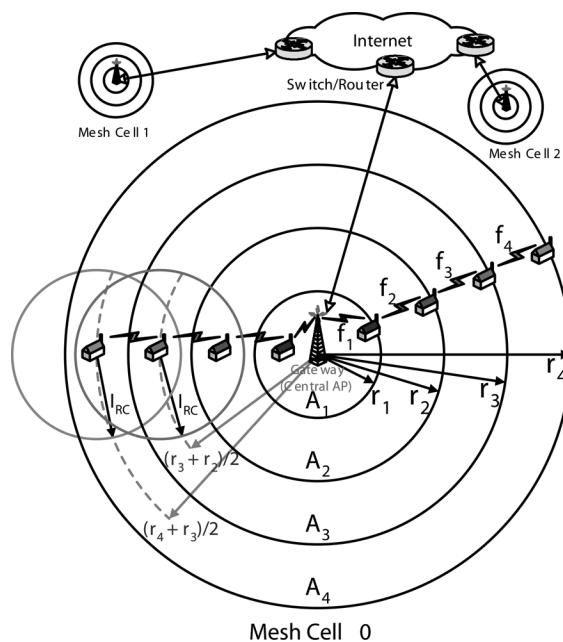


Fig. 1. Mesh cell architecture for a WMN.

a multihop network is to maintain the throughput and QoS while extending the coverage area.

In the literature, the performance issues for WMN have been studied from two directions [1], [2], [6]–[11]. On the one hand, by simulations, authors in [6] demonstrated the coverage advantage of a multihop WMN over a single-hop infrastructure-based network. On the other hand, from a throughput viewpoint, it was shown in [7] and [8] that the user throughput in an ad hoc network is scaled like  $O(1/\sqrt{k \log k})$ , where  $k$  is the total number of users. The authors in [2] pointed out that the achievable user throughput in a WMN will sharply decrease as  $O(1/k)$  due to the bottleneck at the central gateway. Furthermore, the authors in [9]–[11] investigated the throughput and delay tradeoffs in ad hoc networks. These works [9]–[11] addressed the issue whether ad hoc networks can simultaneously achieve high throughput and guarantee the delay requirement. Fewer papers have considered both throughput and coverage performance issues for a WMN, except for [1] in the single-user case. In our previous work [12], the relation of throughput and coverage in a scalable WMN was investigated. However, the QoS issues (i.e., delay and jitter) are not considered in [12].

This paper investigates the optimal tradeoff among capacity, coverage, and QoS for a scalable WMN, as shown in Fig. 1. The proposed WMN is scalable thanks to the following two factors. First, the suggested frequency planning can reduce collisions as cell coverage and users increase. Second, the ring structure can

Manuscript received October 1, 2005; revised March 4, 2006 and May 1, 2006. This work was supported in part by the National Science Council and the Program for Promoting Academic Excellence of Universities under Grant EX-91-E-FA06-4-4, Grant NSC 95-2752-E-009-014-PAE, Grant NSC 94-2213-E-009-030, and Grant NSC 94-2213-E-009-060. This work was presented in part at the IEEE International Conference on Communications (ICC) 2006, Istanbul, Turkey, June 2006.

The authors are with the Department of Communication Engineering, National Chiao-Tung University, Hsinchu 300, Taiwan, R.O.C. (e-mail: hjh@mail.nctu.edu.tw; lichun@cc.nctu.edu.tw; jchang@cc.nctu.edu.tw).

Digital Object Identifier 10.1109/JSAC.2006.881622

facilitate the management of QoS, throughput, and coverage in WMNs. To find the optimal tradeoff among throughput, coverage, and delay, we first develop a physical (PHY)/medium access control (MAC) cross-layer analytical model to evaluate the throughput of the proposed WMN, considering the carrier sense multiple-access (CSMA) MAC protocol, the impact of the ring-based cell structure on frame contentions, and that of hop distance on transmission rate in the physical-layer. Secondly, we develop a queueing model to evaluate the delay and jitter in the considered WMN. Third, we apply the mixed-integer nonlinear programming (MINLP) optimization approach to determine the optimal number of rings in a cell and the associated ring widths, aiming at maximizing the cell capacity and coverage with the QoS requirement.

The rest of this paper is organized as follows. Sections II discusses the proposed network architecture and the impacts of ring-based cell structure on frame contention. In Section III, we formulate an optimization problem to maximize capacity and coverage of a mesh network with a delay constraint. Section IV discusses the channel activity in the ring-based WMN. Section V elaborates the developed cross-layer MAC throughput model for the considered WMN. In Section VI, we analyze the delay and jitter. Numerical examples are shown in Section VII. Concluding remarks and future works are given in Section VIII.

## II. SCALABLE RING-BASED WMN

### A. Network Architecture

Fig. 1 shows the considered ring-based WMN. In the figure, a mesh cell is divided into several rings  $A_i, i = 1, 2, \dots, n$ , determined by  $n$  concentric circles centered at the central gateway with radii  $r_1 < r_2 < \dots < r_n$ . Users in the inner rings will forward data for users in the outer rings toward the central gateway. Accordingly, the user in ring  $A_i$  is connected to the central gateway via an  $i$ -hop communication, and only the gateway connects to the backbone network. Clearly, the cabling engineering work required to deploy this WMN is reduced due to fewer backbone links.

The considered WMN operates in a multichannel fashion. We assume that each node is equipped with two radio interfaces, and therefore can concurrently receive and deliver the forwarded traffic as [3] and [4]. For example, a user in ring  $A_i$  can concurrently communicate with the users in rings  $A_{i-1}$  and  $A_{i+1}$  at two different channels  $f_i$  and  $f_{i+1}$ , respectively. A simple frequency planning is employed to avoid the co-channel interference. The simplicity of the frequency planning lies in the fact that only the width of each ring should be designed to obtain the co-channel reuse distance without interference.

Because the users in the inner rings near the central gateway will relay more traffic than the users in the outer rings, we also sectorize the congested inner rings and allocate different channel to each sector. Since the number of contending users is reduced, the throughput for the ring-based WMN can be further improved. Fig. 2 illustrates an example of a three-cell WMN, where the innermost rings of each cell are divided into three sectors. In this example, the ring-based frequency planning with 12 different channels ensures four buffer rings between

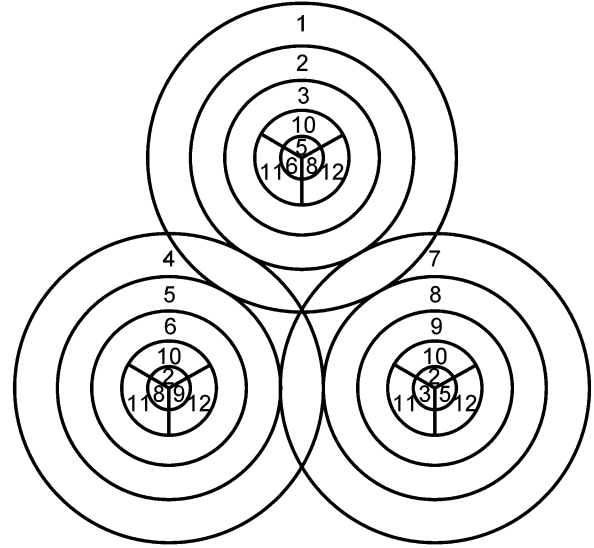


Fig. 2. Example of a three-cell WMN, where the congested rings  $A_1$  and  $A_2$  of each mesh cell are sectorized.

two co-channel rings. Apparently, if more nonoverlapping channels are available, more inner rings can be sectorized to enhance cell capacity and coverage.

### B. Scalability, QoS, and Robustness

Most traditional WMNs are not scalable to cell coverage because throughput and QoS (delay) are not guaranteed with increasing collisions. By contrast, the proposed ring-based WMN is scalable in terms of coverage, because delay and throughput can be ensured by the ring-based frequency planning with appropriately designing the ring widths of the mesh cell. The remaining important problem lies in the way to analytically determine the optimal ring widths so as to achieve the optimal tradeoff among delay, throughput, and coverage.

Due to multiple paths for each node, an appealing feature of WMN is its robustness. If some nodes fail, the mesh network can continue operating with slightly degraded performance by forwarding data traffic via the alternative nodes. Different from the conventional WMNs, the ring-based WMN can easily provide capacity margin for each relay link by decreasing the ring width (and then the hop distance). By doing so, even if some nodes near the central gateway fail, throughput and delay can still be ensured.

### C. Frame Contention Under Ring-Based Cell Structure

To describe frame contention under the ring-based cell structure, we first define the *mutually interfered region* as an area in which any two users can sense the activity of each other. Fig. 3 shows an example of mutually interfered region in ring  $A_i$ , such as the area including nodes  $C$  and  $D$ . Since each ring is allocated with different channel, a mutually interfered region is indeed the intersection of two circles and the associated ring, which is dependent on the locations of observed nodes and the interference distance. For simplicity, we assume that the mutually interfered region in ring  $A_i$  can be approximated as an annulus sector with a central angle of  $\theta_{S,i}$ . Suppose that the interference distance is

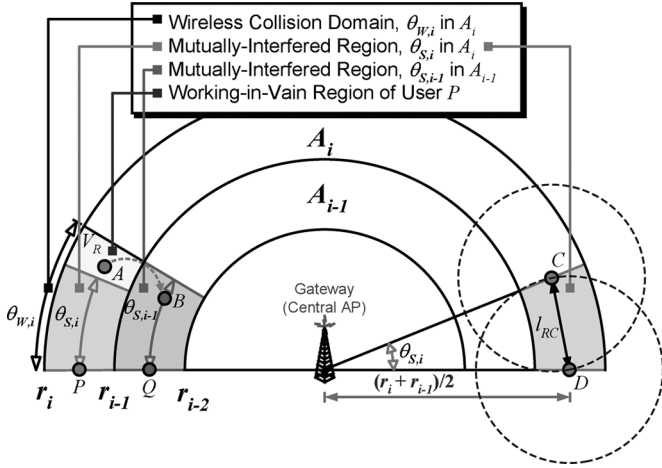


Fig. 3. Examples of wireless collision domain and mutually interfered region.

$l_{RC}$ . Referring to Fig. 3, the central angle  $\theta_{S,i}$  of a mutually interfered region in ring  $A_i$  is equal to

$$\theta_{S,i} = 2 \sin^{-1} \left( \frac{l_{RC}}{r_i + r_{i-1}} \right), \quad \text{for } l_{RC} < (r_i + r_{i-1}). \quad (1)$$

If  $l_{RC} \geq (r_i + r_{i-1})$ , we define  $\theta_{S,i} = 2\pi$  which means that the whole ring is in the same mutually interfered region. Clearly, the area of a mutually interfered region is  $A_{S,i} = (\theta_{S,i}/2\pi)a_i$  and  $a_i = \pi(r_i^2 - r_{i-1}^2)$  is the area of ring  $A_i$ .

Then, we define the *wireless collision domain* as the area in which at any instant at most one user can successfully transmit data traffic at a particular frequency. Referring to Fig. 3, the wireless collision domain in ring  $A_i$  is also approximated as an annulus sector with a central angle of  $\theta_{W,i} = \theta_{S,i-1}$ , and its area is  $A_{W,i} = (\theta_{W,i}/2\pi)a_i$ . The phenomenon of  $\theta_{W,i} = \theta_{S,i-1}$  is due to the fact that the four-way handshaking request-to-send/clear-to-send (RTS/CTS) mechanism is employed to avoid the hidden node problem. As the example in Fig. 3, user  $A$  in ring  $A_i$  is sending data to user  $B$  in ring  $A_{i-1}$ . After the RTS/CTS exchange, node  $Q$  in ring  $A_{i-1}$  determines that the channel is busy. In the meantime, since users  $P$  and  $A$  belong to different mutually interfered regions, user  $P$  in ring  $A_i$  can send an RTS frame to users  $Q$ . Nevertheless, user  $Q$  will not reply the CTS frame to  $P$  because it has overheard the CTS of  $B$ . As a result, nodes  $P$  and  $A$  are in the same wireless collision domain even though they are not in the same mutually interfered region. This fact means that the central angle  $\theta_{W,i}$  of wireless collision domain in ring  $A_i$  is determined by the angle  $\theta_{S,i-1}$  of mutually interfered region in the inner ring  $A_{i-1}$ . That is,  $\theta_{W,i} = \theta_{S,i-1}$ .

The example in Fig. 3 also shows that the existence of transmitters in region  $V_R$  invalidates the RTS request of  $P$ . Hence, we define the region  $V_R$  with a central angle of  $(\theta_{W,i} - \theta_{S,i})$  as the *working-in-vain region* of  $P$ . Such an impact of the ring structure on frame contention will be incorporated into the cross-layer throughput model later.

In addition, note that the innermost ring  $A_1$  is in the same wireless collision domain and  $\theta_{W,1} = 2\pi$ , since all users in ring  $A_1$  can overheard the CTS frame from the central AP. After sectorizing ring  $A_1$  as shown in Fig. 2, the number of contending

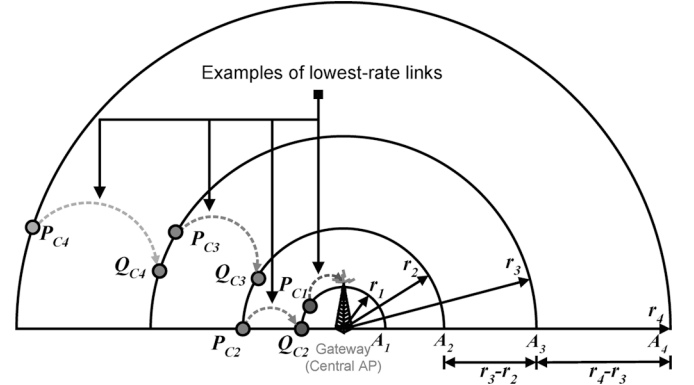


Fig. 4. Examples of the lowest rate links for a mesh cell with  $n = 4$ .

users is decreased by a factor of three since  $\theta_{W,1} = 2\pi/3$ . Similarly, we can further sectorize ring  $A_2$ , which will help resolve the bottleneck issue in this multihop network.

### III. CAPACITY AND COVERAGE MAXIMIZATION

#### A. Problem Formulation

All the performance issues of throughput, coverage, and QoS will impact the design of WMNs. From the viewpoint of deployment cost, a larger coverage per cell is better because of fewer access points. From the standpoint of throughput, however, a smaller cell is preferred since fewer users contend for the same radio channel. This paper mainly focuses on frame delay consisting of contention delay and queuing delay in each relay node. From the queuing delay perspective, a longer hop distance may be better due to fewer hops. From the contention delay viewpoint, however, a shorter hop distance is preferred due to fewer contending users. In the following, we formulate an optimization problem to determine the best number of rings in a cell and the optimal ring widths subject to the constraints on delay, throughput, and coverage.

To begin with, we discuss the constraints in the considered optimization problem.

- The capacity  $H_C(i)$  of the lowest-rate link in ring  $A_i$  should be greater than the carried traffic load  $R_i$  of each node, i.e.,

$$H_C(i) = H_i(r_i - r_{i-1}) \geq R_i \quad (2)$$

where  $(r_i - r_{i-1})$  is the width of ring  $A_i$  and  $H_i(d)$  represents the link capacity between two nodes at a separation distance  $d$ . This constraint guarantees the minimum throughput for each user. As shown in Fig. 4, the lowest-rate link in ring  $A_i$  is the link between nodes  $P_{C,i}$  and  $Q_{C,i}$  at a separation distance  $d = (r_i - r_{i-1})$ .

- The overall frame delay  $D_f$  should meet the delay requirement  $D_{req}$ , i.e.,

$$D_f \leq D_{req}. \quad (3)$$

- The ring width ( $r_i - r_{i-1}$ ) should be less than the maximum reception range

$$(r_i - r_{i-1}) \leq d_{\max} = d_1. \quad (4)$$

- The ring width should be greater than the average distance  $d_{\min}$  between two neighboring nodes, i.e.,

$$(r_i - r_{i-1}) \geq d_{\min} \quad (5)$$

where  $d_{\min} = 1/\sqrt{\rho}$  (m) is dependent on the user node density  $\rho$ . This constraint also represents the limit on the hop distance due to node density.

### B. MINLP Optimization Approach

From the above considerations, the optimal capacity and coverage issues in a WMN can be formulated as a MINLP problem with the following decision variables:  $n$  (the number of rings in a mesh cell) and  $r_1, r_2, \dots, r_n$ . The objective function is to maximize the capacity of a mesh cell. In this scalable ring-based WMN, the ring-based frequency planning resolves the collision issue as cell coverage increases. Accordingly, the optimal coverage and capacity will be achieved simultaneously, since more users in a mesh cell can also lead to higher cell capacity. The optimal system parameters for the ring-based WMN can be analytically determined by solving the following optimization problem:

$$\begin{aligned} & \text{MAX} \\ & n, r_1, r_2, \dots, r_n \quad \rho \pi r_n^2 R_D \end{aligned} \quad \text{(Overall throughput of a mesh cell)}$$

subject to

$$H_C(i) \geq R_i \quad (6)$$

$$D_f \leq D_{\text{req}} \quad (7)$$

$$d_{\max} \geq (r_i - r_{i-1}) \geq d_{\min} \quad (8)$$

where  $\rho$  is the user density, and  $R_D$  is the traffic load generated by each user.

## IV. CHANNEL ACTIVITY IN THE RING-BASED WMN

From the viewpoint of a particular user, there are five types of channel activities in the considered ring-based WMN.

- 1) Successful frame transmission.
- 2) Unsuccessful frame transmission.
- 3) Empty slot, where all users are in backoff or idle.
- 4) Successful frame transmission from other users.
- 5) Unsuccessful frame transmission from other users.

For clarity, the activity of a radio channel is described by a sequence of *effective time slots* [13]–[15]. Subject to the backoff procedures, their durations are defined as

$$\begin{cases} T_1 = T_4 = T_S \\ T_2 = T_5 = T_C \\ T_3 = \sigma \end{cases} \quad (9)$$

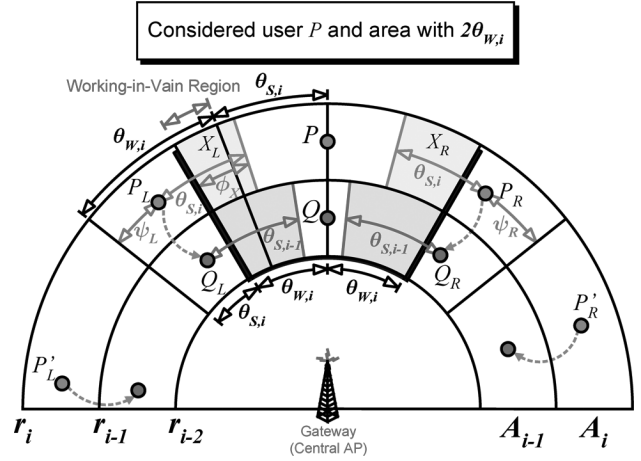


Fig. 5. The considered user  $P$  and two adjacent wireless collision domains, where user  $P$  is contending for the radio channel.

where  $\sigma$  is the duration of an empty slot,  $T_S$  and  $T_C$  are the successful transmission time and collision duration, respectively. Therefore, the average duration  $T_v$  of an effective time slot can be written as

$$T_v = \sum_{j=1}^5 \nu_j T_j. \quad (10)$$

Here,  $\nu_j$  is the corresponding probability for the channel activity type as calculated in the following, and  $\sum_{j=1}^5 \nu_j = 1$ .

### A. Successful/Unsuccessful Transmission

In Fig. 5, user  $P$  can successfully send data as long as no other user is transmitting in the adjacent wireless collision domains of  $P$ . Consider user  $P$  and its two wireless collision domains influenced by two closest neighboring transmitters  $P_L$  and  $P_R$ , which are out of the mutually interfered regions of  $P$ , as shown in Fig. 5.<sup>1</sup> Let  $\psi_L$  and  $\psi_R$  be the positions of  $P_L$  and  $P_R$ , respectively. If one of the transmitters  $P_L$  and  $P_R$  is within the working-in-vain regions of  $P$ , i.e.,  $\psi_L, \psi_R \in [\theta_{S,i}, \theta_{W,i}]$ , user  $P$  can still send the RTS request to user  $Q$ , but user  $Q$  cannot reply the CTS acknowledgment (ACK), as discussed in Section II-C. Suppose that  $Z_{W,i}$  is the average probability (average fraction of time) of a wireless collision domain in which a user is delivering data, as defined in (33). Then, the working-in-vain probability  $p_v$  of user  $P$  can be expressed as

$$\begin{aligned} p_v &= 1 - \Pr \{ \psi_L, \psi_R \notin [\theta_{S,i}, \theta_{W,i}] \} \\ &= 1 - \left[ 1 - Z_{W,i} \frac{\theta_{W,i} - \theta_{S,i}}{\theta_{W,i}} \right]^2 \end{aligned} \quad (11)$$

where note that  $Z_{W,i}$  accounts for the existence probability of transmitter  $P_L$  ( $P_R$ ) which is affecting the considered area.

<sup>1</sup>In this ring-based WMN, the considered area of angle  $2\theta_{W,i}$  will be influenced by at most two neighboring transmitters (e.g., nodes  $P_L$  and  $P_R$  in Fig. 5). Other transmitters (e.g., nodes  $P'_L$  and  $P'_R$ ) are too far away, and will not affect the considered area.

Now, we consider the case that both transmitters  $P_L$  and  $P_R$  are not in the working-in-vain regions of user  $P$ , i.e.,  $\psi_L, \psi_R \in [0, \theta_{S,i}]$ . In the considered area of angle  $2\theta_{W,i}$ , only the users in the area  $\{2A_{W,i} - (X_L + X_R)\}$  can send RTS frames, as shown in Fig. 5. Those users in regions  $X_L$  and  $X_R$  will not send their requests since they can sense the transmissions of  $P_L$  and  $P_R$ . Let  $\bar{\phi}_X$  be the average central angle for region  $X_L$ , and  $A_{W,i}$  be the area of a wireless collision domain of user  $P$ .

Therefore, the average number of contending users in the considered area of angle  $2\theta_{W,i}$  is equal to the average number of users in the area of  $\{2A_{W,i} - (X_L + X_R)\}$ , i.e.,

$$\begin{aligned} c_{1,i} &= \frac{\rho a_i}{2\pi} 2(\theta_{W,i} - Z_{W,i} \bar{\phi}_X) \\ &= \frac{\rho a_i}{\pi} \left( \theta_{W,i} - \frac{Z_{W,i}}{\theta_{W,i}} \int_0^{\theta_{S,i}} \psi_L d\psi_L \right) \\ &= \rho (r_i^2 - r_{r-1}^2) \left( \theta_{W,i} - \frac{Z_{W,i} \theta_{S,i}^2}{2\theta_{W,i}} \right) \end{aligned} \quad (12)$$

where  $\rho$  is the user density;  $a_i = \pi(r_i^2 - r_{i-1}^2)$  is the area of ring  $A_i$ ;  $\theta_{S,i}$  is the central angle of the mutually interfered region, as defined in (1);  $\phi_X = (\psi_L + \theta_{S,i}) - \theta_{S,i} = \psi_L$  is the central angle of region  $X_L$  and  $\psi_L$  is uniformly distributed in  $[0, \theta_{W,i}]$ , as shown in Fig. 5. Subject to the RTS/CTS procedures, the frame collisions may only occur when the contending users concurrently deliver their RTS requests. Let  $\tau$  be the average probability of an active user sending the RTS request at the beginning of an effective slot. Suppose that  $P_0$  is the average probability of a user being idle due to empty queue. Incorporating the impacts of ring structure on frame contention, the unsuccessful transmission probability  $p_u$  can be computed by

$$p_u = p_v + (1 - p_v)[1 - (1 - \tau(1 - P_0))^{c_{1,i}-1}]. \quad (13)$$

In (13), the first term is the probability that at least one transmitter is inside the working-in-vain regions of  $P$ . That is, user  $P$  will not receive the CTS response. The second term represents the probability that the RTS request from  $P$  is collided with other RTS frames.

Thus, given that the considered user has a nonempty queue, the probability that this user successfully/unsuccessfully sends data frame in an effective slot can be expressed as

$$\nu_1 = \tau(1 - p_u) \quad (14)$$

$$\nu_2 = \tau p_u. \quad (15)$$

### B. Empty Slot

In Fig. 6, user  $P$  observes an empty slot if all the users in the adjacent mutually interfered regions of user  $P$  are silent. As shown in the figure, the users in regions  $Y_L$  and  $Y_R$  will not send RTS due to the transmissions of  $P_L$  and  $P_R$ . Let  $\bar{\phi}_Y$  be the average central angle of region  $Y_L$ , and  $A_{S,i}$  be the area of a mutually interfered region of user  $P$ . The average number of contending users in the considered area of angle  $2\theta_{S,i}$  is equal to

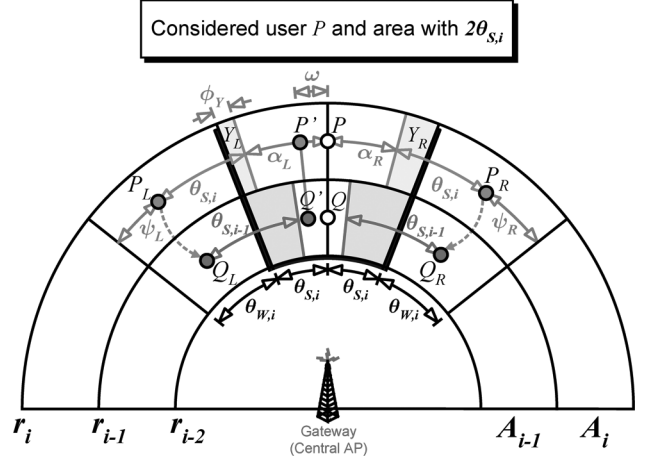


Fig. 6. The considered user  $P$  and its two mutually interfered regions, where user  $P$  is in backoff at the current slot.

the average number of users in the area of  $\{2A_{S,i} - (Y_L + Y_R)\}$ , i.e.,

$$\begin{aligned} c_{2,i} &= \frac{\rho a_i}{2\pi} 2(\theta_{S,i} - Z_{W,i} \bar{\phi}_Y) \\ &= \frac{\rho a_i}{\pi} \left( \theta_{S,i} - \frac{Z_{W,i}}{\theta_{W,i}} \int_0^{\theta_{W,i}} \max(0, \psi_L + \theta_{S,i} - \theta_{W,i}) d\psi_L \right) \\ &= \rho (r_i^2 - r_{r-1}^2) \left( \theta_{S,i} - \frac{Z_{W,i} \theta_{S,i}^2}{2\theta_{W,i}} \right) \end{aligned} \quad (16)$$

where  $\phi_Y = \max(0, \psi_L + \theta_{S,i} - \theta_{W,i})$  is the central angle of region  $Y_L$ , as shown in Fig. 6. Accordingly, from the viewpoint of the considered user, the empty-slot probability is

$$\nu_3 = (1 - \tau)[1 - \tau(1 - P_0)]^{c_{2,i}-1} \quad (17)$$

where the first term is the probability of the considered user being in backoff, and the second term represents the probability that all the other users are in backoff or idle.

### C. Successful/Unsuccessful Transmission From Other Users

To calculate the successful transmission probability from other users, we consider user  $P$  and its two mutually interfered regions, as shown in Fig. 6. In the considered area of angle  $2\theta_{S,i}$ , the average number of contending users is  $c_{2,i}$  as derived in (16). Given that user  $P$  is in backoff at the current slot, the probability that at least one user sends RTS is equal to  $p_{otr} = 1 - [1 - \tau(1 - P_0)]^{c_{2,i}-1}$ . Suppose that  $X_j$  is the probability of the considered area being influenced by  $j$  neighboring transmitters. Consequently, in the considered area of angle  $2\theta_{S,i}$ , the conditional probability that there is at least one successful transmission from other users is expressed as

$$p_{os} = \frac{\sum_{j=0}^2 (2s_{1,j} - s_{2,j}) X_j}{p_{otr}} \quad (18)$$

where  $X_j = \binom{2}{j} Z_{W,i}^j (1 - Z_{W,i})^{2-j}$ ,  $s_{1,j}$  is the probability that the left-side mutually interfered region of user  $P$  contains a successful transmission, and  $s_{2,j}$  is the probability that each mutually interfered region of  $P$  contains a successful transmission. Then, from the viewpoint of the considered user, the probability of an effective slot containing successful/unsuccessful transmission(s) from other users can be expressed as

$$\nu_4 = (1 - \tau)p_{\text{otr}}p_{\text{os}} \quad (19)$$

$$\nu_5 = (1 - \tau)p_{\text{otr}}(1 - p_{\text{os}}). \quad (20)$$

The successful probabilities  $s_{1,j}$  and  $s_{2,j}$  will be derived in the appendix.

## V. CROSS-LAYER THROUGHPUT ANALYSIS

This section suggests an analytical throughput model for the ring-based mesh network using the CSMA MAC protocol with RTS/CTS. Although the 802.11a wireless local area network (WLAN) is used as an example here, the developed analytical framework can be applied to various wireless systems, e.g., the IEEE 802.11/15/16 networks, as well as the free-space optics (FSO) systems [16].

### A. Background

Now, we calculate the duration of a successful frame transmission and a collision in the IEEE 802.11a network. Let  $l$  be the payload size of data frame,  $m_a$  and  $m_c$  be the transmission PHY mode for data frames and that for control frames, respectively. Subject to the IEEE 802.11 CSMA MAC protocol with RTS/CTS, the successful frame transmission time  $T_S$  and collision time  $T_C$  are expressed as

$$\begin{aligned} T_S &= T_{\text{RTS}}(m_c) + \delta + \text{SIFS} + T_{\text{CTS}}(m_c) + \delta + \text{SIFS} \\ &\quad + T_{\text{DATA}}(l, m_a) + \delta + \text{SIFS} \\ &\quad + T_{\text{ACK}}(m_c) + \delta + \text{DIFS} \end{aligned} \quad (21)$$

$$T_C = T_{\text{RTS}}(m_c) + \delta + \text{EIFS} \quad (22)$$

where  $\delta$  is the propagation delay; the durations of short interframe space (SIFS), distributed interframe space (DIFS), and extended interframe space (EIFS = SIFS +  $T_{\text{CTS}}(m_c)$  + DIFS) are specified in [17]. [18].

In the IEEE 802.11a WLAN [18], a data frame includes the physical-layer convergence procedure (PLCP) sublayer preamble (PLCP<sub>pre</sub>), PLCP SIGNAL field (PLCP<sub>SIGNAL</sub>), 16-bit SERVICE field in the PLCP header and six tail bits, MAC header (MAC<sub>hdr</sub>), as well as frame check sequence field (MAC<sub>FCS</sub>). The transmission time  $T_{\text{DATA}}(l, m_a)$  for a data frame with payload size  $l$  using PHY mode  $m_a$  is given as

$$\begin{aligned} T_{\text{DATA}}(l, m_a) &= \text{PLCP}_{\text{pre}} + \text{PLCP}_{\text{SIGNAL}} \\ &\quad + \left[ \frac{\text{MAC}_{\text{hdr}} + \text{MAC}_{\text{FCS}} + (16 + 6)/8 + l}{\text{NBpS}(m_a)} \right] \cdot T_{\text{SYM}} \\ &= 20\mu\text{s} + \left[ \frac{30.75 + l}{\text{NBpS}(m_a)} \right] \cdot 4\mu\text{s} \end{aligned} \quad (23)$$

where  $\text{NBpS}(\cdot)$  is the number of data bytes in an OFDM symbol, and  $T_{\text{SYM}}$  is an OFDM symbol duration. For RTS, CTS, and ACK control frames using PHY mode  $m_c$ , their transmission durations can be written as

$$\begin{aligned} T_{\text{RTS}}(m_c) &= \text{PLCP}_{\text{pre}} + \text{PLCP}_{\text{SIGNAL}} \\ &\quad + \left[ \frac{\text{RTS} + (16 + 6)/8}{\text{NBpS}(m_c)} \right] \cdot T_{\text{SYM}} \end{aligned} \quad (24)$$

$$\begin{aligned} T_{\text{CTS}}(m_c) &= T_{\text{ACK}}(m_c) \\ &= \text{PLCP}_{\text{pre}} + \text{PLCP}_{\text{SIGNAL}} \\ &\quad + \left[ \frac{\text{ACK} + (16 + 6)/8}{\text{NBpS}(m_c)} \right] \cdot T_{\text{SYM}} \end{aligned} \quad (25)$$

where RTS and ACK are the lengths of RTS and ACK frames, respectively.

### B. Carried Traffic Load of a User Node

The carried traffic load in each mesh node includes its own traffic and the forwarded traffic from other users. Assume that all the nodes in the inner ring  $A_i$  share the relayed traffic from the outer ring  $A_{i+1}$ . Suppose that the user density is  $\rho$ . The average number of nodes  $c_i$  in ring  $A_i$  can be expressed as

$$c_i = \rho a_i = \begin{cases} \rho \pi r_i^2, & \text{for } i = 1 \\ \rho \pi (r_i^2 - r_{i-1}^2), & \text{for } 1 < i \leq n \end{cases} \quad (26)$$

where  $a_i$  and  $(r_i - r_{i-1})$  are the area and the width of ring  $A_i$ , respectively. Let  $R_D$  and  $R_i$  represent traffic load generated by each node and the total carried traffic load per node in ring  $A_i$ , respectively. Then, it is followed that

$$R_i = \frac{c_{i+1}}{c_i} R_{i+1} + R_D = \left[ \frac{\sum_{j=i+1}^n c_j}{c_i} + 1 \right] R_D. \quad (27)$$

For the outermost ring  $A_n$ ,  $R_n = R_D$ .

### C. MAC Throughput

To evaluate the MAC throughput in the ring-based WMN, we should consider the impacts of the physical-layer ring structure on frame contention. Consider a binary exponential backoff procedure with the initial backoff window size of  $W$ . Let  $m_{\text{bk}}$  be the maximum backoff stage. The average backoff time can be calculated by

$$\begin{aligned} \overline{B}_k &= (1 - p_u) \frac{W - 1}{2} + p_u (1 - p_u) \frac{2W - 1}{2} + \dots \\ &\quad + p_u^{m_{\text{bk}}} (1 - p_u) \frac{2^{m_{\text{bk}}} W - 1}{2} \\ &\quad + p_u^{(m_{\text{bk}}+1)} (1 - p_u) \frac{2^{m_{\text{bk}}} W - 1}{2} + \dots \\ &= \frac{[1 - p_u - p_u (2p_u)^{m_{\text{bk}}}] W - (1 - 2p_u)}{2(1 - 2p_u)} \end{aligned} \quad (28)$$

where  $p_u$  is the unsuccessful transmission probability with considering the impacts of ring structure in the physical layer, as defined in (13). Since a user sends RTS requests every  $(\overline{B}_k + 1)$

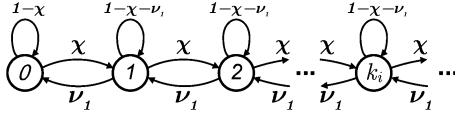


Fig. 7. State transition diagram for the considered user, where the state variable  $k_i$  is the number of frames queued at the considered user.

slots on average [19], the transmission probability  $\tau$  for an active user can be written as

$$\tau = \frac{1}{B_k + 1} = \frac{2}{1 + W + p_u W \sum_{i=0}^{m_{bk}-1} (2p_u)^i}. \quad (29)$$

From (13) and (29), we can obtain the unique solution of  $\tau$  and  $p_u$  for a given idle probability  $P_0$  of a user. The idle probability  $P_0$  will be derived by the following queueing model.

Fig. 7 illustrates the proposed discrete-time queueing model for a user in ring  $A_i$ , where the state variable  $k_i$  represents the number of frames queued in the user. In each effective time slot, the probability for one user to successfully transmit a data frame is  $\nu_1$ , as defined in (14). Consequently, the total contention delay spent for a frame (i.e., the frame service time) is a geometric random variable with a mean of  $1/\nu_1$  effective slots. In a multihop network, this phenomenon means that the arrival process of relayed traffic is also Markovian since the interarrival time of relayed traffic is geometrically distributed. Let  $l$  be the payload size of data frame. It is reasonable to assume that the frame arrivals at one user follow a Poisson process with a rate of  $\lambda = R_i/l$  frames/s. Here,  $R_i$  is the total carried traffic load of a user in ring  $A_i$ , including the local traffic of user and the forwarded traffic from others. From above considerations, the state-transition probabilities for the queueing model can be defined as

$$\begin{cases} p_{k,k+1} = \chi = \lambda T_v \\ p_{k,k-1} = \nu_1 \\ p_{k,k} = 1 - \chi - \nu_1. \end{cases} \quad (30)$$

Therefore, the state probability can be obtained as

$$P_k = u_c^k (1 - u_c) \quad (31)$$

where  $u_c = \chi/\nu_1$  and the idle probability of a user can be given as  $P_0 = (1 - u_c)$ .

Now, we evaluate the MAC throughput of one user. With the effective slot concept, the average busy probability (average fraction of time)  $Z_{O,i}$  of one user being sending data and the channel utilization  $Z_{W,i}$  of a wireless collision domain can be expressed as

$$Z_{O,i} = \frac{\nu_1 T_1 (1 - P_0)}{T_v} \quad (32)$$

$$Z_{W,i} = \rho A_{W,i} Z_{O,i} \quad (33)$$

where  $\nu_1$  is the probability that one user successfully sends a frame in an effective slot,  $T_1 = T_S$  is the time duration for successful frame transmission,  $T_v$  is the average duration of an effective slot, and  $\rho A_{W,i}$  is the number of users in a wireless

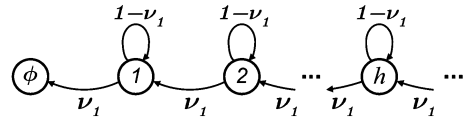


Fig. 8. State transition diagram for the considered frame in a user, where the state variable  $h$  means the considered frame being placed at the  $(h+1)$  position of the queue.

collision domain. From (10), (14), and (31)–(33),  $\nu_1$ ,  $T_v$ , and  $P_k$  can be calculated by an iterative method. Then, the capacity  $H_i(d)$  of a mesh link between two nodes at a separation distance  $d$  can be calculated by

$$H_i(d) = \frac{\nu_1 T_1}{T_v} \cdot \frac{l}{T_S} = \frac{\nu_1 l}{T_v} \quad (34)$$

where  $l$  is the payload size of data frame. It is noteworthy that the payload size  $l$  of data frame is affected by the separation distance  $d$  and the PHY mode  $m_a$ , which will be discussed in the next section.

#### D. Impact of Hop Distance on Transmission Rate

In a multihop network, the hop distance will also impact the throughput of relay link. Generally, the radio signal is affected by path loss, shadowing, as well as multipath fading. With all these radio channel effects, we assume that the average reception ranges for eight PHY modes are  $d_j$ ,  $j = 1, 2, \dots, 8$ , where  $d_1 > d_2 > \dots > d_8$ . In principle, two users with a shorter separation distance can transmit at a higher data rate. Therefore, the transmission PHY mode  $m_a$  is determined according to the separation distance  $d$  between two users, i.e.,

$$m_a = j, \quad \text{if } d_{j+1} < d \leq d_j. \quad (35)$$

Furthermore, we suggest that all data frames have the same transmission time  $T_{\text{DATA}}(l, m_a)$ . That is, the payload size  $l$  of data frame is determined by the adopted PHY mode  $m_a$ . As in [20] and [21], the same transmission time for each data frame can achieve fairness and avoid throughput degradation due to low-rate transmissions.

## VI. DELAY ANALYSIS

This section presents an analytical method to evaluate the delay and jitter (delay variance) of a Markov process, without the need to derive the probability distribution of delay as in [22]. Consider a frame being placed at the  $h$ th position of the first-come, first-serve (FCFS) queue of a user. The state-transition diagram for the considered frame is illustrated in Fig. 8, which is obtained from the model in Fig. 7 by withdrawing the state transitions due to frame arrivals. In the figure, state  $h = 1$  represents the one that the considered frame is contending for the radio channel in the current effective slot. Moreover, state  $h = \phi$  is defined as the one that the considered frame is successfully delivered. Let  $I_h = h'$  be the state transition from state  $h$  to state  $h'$  in an effective slot. Then, the state-transition probability can be expressed as

$$\Pr[I_h = h'] = \begin{cases} \nu_1, & \text{for } h' = (h-1) \\ (1 - \nu_1), & \text{for } h' = h \end{cases}. \quad (36)$$

Now, we deal with the time  $D_h$  spent for a frame to enter state  $\phi$  (i.e., be successfully transmitted) given that this frame is now at state  $h$ . Clearly,

$$E[D_h | I_h] = \begin{cases} 1 + E[D_{h-1}], & \text{for } I_h = (h-1) \\ 1 + E[D_h], & \text{for } I_h = h \end{cases} \quad (37)$$

where  $D_h$  is expressed in effective slots. Therefore, the mean of  $D_h$  is equal to

$$\begin{aligned} E[D_h] &= \sum_{I_h} \Pr[I_h] E[D_h | I_h] \\ &= 1 + \nu_1 E[D_{h-1}] + (1 - \nu_1) E[D_h]. \end{aligned} \quad (38)$$

Since  $E[D_1] = 1/\nu_1$ , from (38), we can obtain

$$E[D_h] = \frac{1}{\nu_1} + E[D_{h-1}] = \frac{h}{\nu_1}. \quad (39)$$

By the conditional variance formula, the variance of  $D_h$  can be expressed as

$$\text{Var}(D_h) = \text{Var}(E[D_h | I_h]) + E[\text{Var}(D_h | I_h)]. \quad (40)$$

From (37), it is followed that

$$\begin{aligned} \text{Var}(E[D_h | I_h]) &= \sum_{I_h} \Pr[I_h] E[D_h | I_h]^2 - (E[D_h])^2 \\ &= \frac{1}{\nu_1^2} - 1. \end{aligned} \quad (41)$$

In addition, it is obvious that

$$E[\text{Var}(D_h | I_h)] = \nu_1 \text{Var}(D_{h-1}) + (1 - \nu_1) \text{Var}(D_h). \quad (42)$$

From (40) to (42) with some manipulations, we can obtain

$$\text{Var}(D_h) = \frac{1 - \nu_1}{\nu_1^2} + \text{Var}(D_{h-1}) = \frac{h(1 - \nu_1)}{\nu_1^2} \quad (43)$$

where the initial condition is  $\text{Var}(D_1) = (1 - \nu_1)/\nu_1^2$ .

Hence, the mean  $D(i)$  and variance  $\sigma_D^2(i)$  of the sojourn time for a frame spent in a relay node can be calculated by

$$\begin{aligned} D(i) &= E[E[D_h]] = \sum_{h=1}^{\infty} Q_h E[D_h] \\ &= \sum_{h=1}^{\infty} u_c^{h-1} (1 - u_c) E[D_h] = \frac{1}{\nu_1(1 - u_c)} \quad (44) \\ \sigma_D^2(i) &= \text{Var}(E[D_h]) + E[\text{Var}(D_h)] \\ &= \sum_{h=1}^{\infty} u_c^{h-1} (1 - u_c) E[D_h]^2 - [D(i)]^2 \\ &\quad + \sum_{h=1}^{\infty} u_c^{h-1} (1 - u_c) \text{Var}(D_h) \\ &= \frac{1 - \nu_1(1 - u_c)}{\nu_1^2(1 - u_c)^2} \end{aligned} \quad (45)$$

TABLE I  
SYSTEM PARAMETERS FOR NUMERICAL EXAMPLES

Symbol	Item	Nominal value
$\rho$	User node density	$(100)^{-2} \text{m}^{-2}$
$R_D$	Demanded traffic of each user	0.5 Mbps
$d_{min}$	Min. of ring width, i.e., $(1/\sqrt{\rho})$	100 (m)
$d_{max}$	Max. reception range	300 (m)
$l_{RC}$	Interference distance $(\gamma_I d_{max})$	450 (m)

where  $u_c = \chi/\nu_1$  and  $Q_h = P_{h-1} = u_c^{h-1}(1 - u_c)$  represents the probability of having  $(h-1)$  frames queued in the relay node at the instant a data frame arrives.

In a multihop network, the overall frame delay is defined as the elapsed time from the frame generated at the source node to the successful reception by the central AP. Consider a frame generated at a node in the outermost ring  $A_n$ . Then, the mean and variance of overall delay for the considered frame can be calculated from

$$D_f = \sum_{i=1}^n D(i) \quad (46)$$

$$\sigma_{D_f}^2 = \sum_{i=1}^n \sigma_D^2(i) \quad (47)$$

where  $n$  is the number of rings in a mesh cell.

## VII. NUMERICAL RESULTS

In this section, we investigate the interactions among delay, capacity and coverage in a ring-based WMN. The numerical results are analytically derived by means of the proposed cross-layer analytical model and the MINLP optimization approach. The system parameters are summarized in Table I. The RTS/CTS/ACK control frames are transmitted with PHY mode  $m_c = 1$  for reliability. We assume the interference distance  $l_{RC} = \gamma_I d_{max}$ , where  $\gamma_I$  is 1.5. As in [20], the chosen frame payload sizes for eight PHY modes are {425, 653, 881, 1337, 1793, 2705, 3617, 4067} bytes. Referring to the measured results [23], the corresponding average reception ranges are  $d_j = \{300, 263, 224, 183, 146, 107, 68, 30\}$  meters. These reception ranges may vary for different environments. However, the proposed optimization approach is general enough for different WMNs with various reception ranges.

### A. Interactions Among Delay, Capacity, and Coverage

Figs. 9–11 investigate the interactions among the delay, capacity, and coverage, where both rings  $A_1$  and  $A_2$  are sectorized. Fig. 9 illustrates the coverage performance against the number of rings  $n$  in a mesh cell under different delay requirements. In the figure, it is obvious that the optimal cell coverage slightly decreases from 610 to 603 (m) at  $n = 5$  to meet the delay requirement  $D_{req} = 0.1$  (s). However, for a more stringent delay requirement  $D_{req} = 0.01$  (s), the optimal cell coverage will diminish to 488 (m) at  $n = 4$ .

Fig. 9 also shows that the number of rings  $n$  in a cell has a maximum value. In general, when  $n$  increases, cell coverage

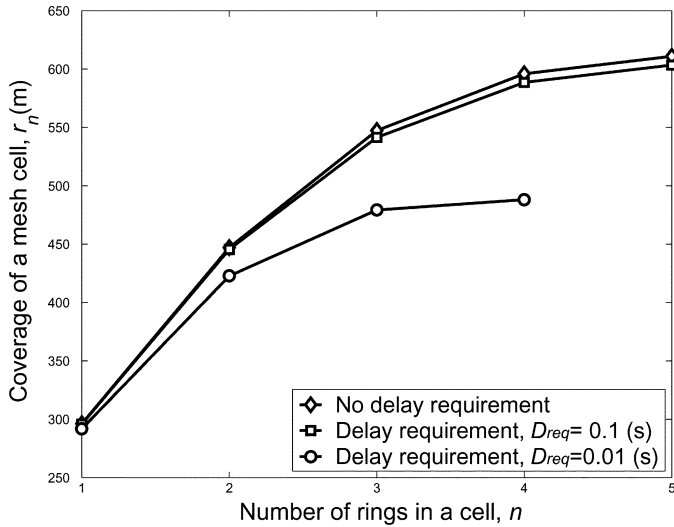


Fig. 9. Cell coverage versus the number of rings  $n$  in a cell under different delay requirements, where the demanded traffic per user is  $R_D = 0.5$  (Mb/s).

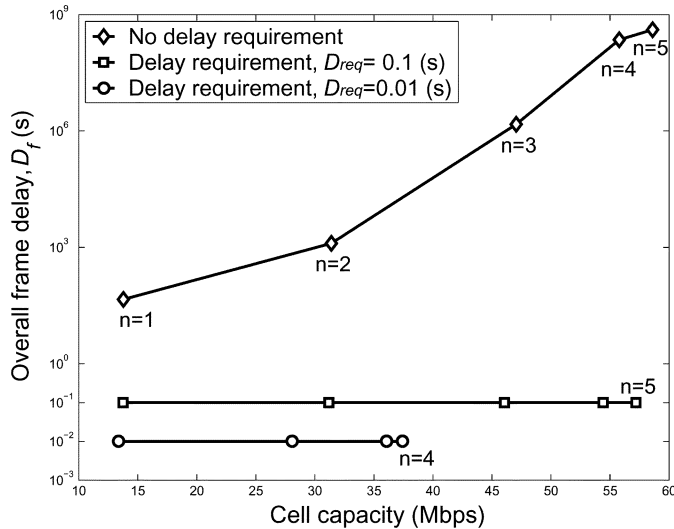


Fig. 10. Overall frame delay  $D_f$  versus cell capacity under different delay requirements.

also increases. For handling the increasing relay traffic as  $n$  increases, the ring width will be reduced to shorten the hop distance, thereby improving the link capacity. However, because the minimum allowable ring width is determined by the node density according to (8), there will exist a maximum value of  $n$ . In this example, the maximum allowable number of rings in a cell is  $n = 4$  for the case with delay requirement  $D_{req} = 0.01$ , and  $n = 5$  for the other cases.

In Fig. 10, the overall frame delay  $D_f$  versus cell capacity under different delay requirements is shown. The frame delay can be dramatically improved from  $4 \times 10^8$  to 0.1 (s) at  $n = 5$ , while the optimal cell throughput merely decreases from 58.6 to 57.2 Mb/s. The phenomenon of extreme delay is due to the fact that the link is fully utilized if without any delay constraint. From (44), for  $u_c \approx 1$ , the sojourn time of data frame will grow toward a very large value [22]. However, by shortening the hop distance, we can raise the link capacity to improve delay performance at the expense of a smaller cell coverage, as shown in

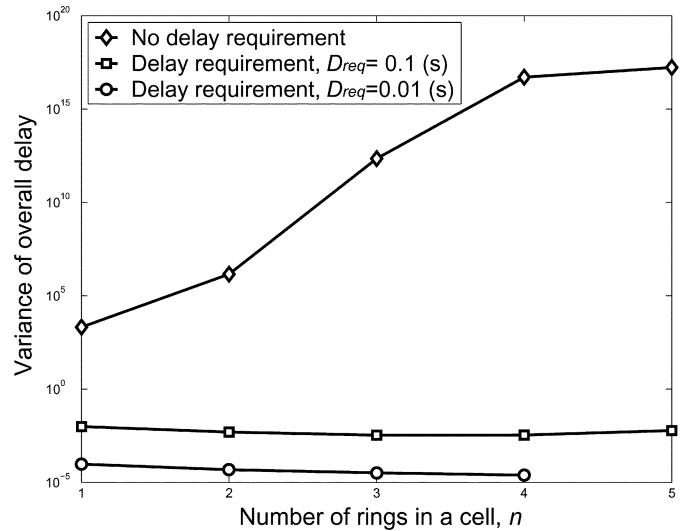


Fig. 11. Overall delay variance (jitter) versus the number of rings  $n$  in a cell under different delay requirements.

Fig. 9. From Fig. 10, one can also see that the delay requirement  $D_{req} = 0.01$  (s) is fulfilled at the expense that the optimal cell capacity decreases to 37.4 Mb/s at  $n = 4$ .

Fig. 11 shows the variance of overall delay (jitter) against the number of rings subject to various delay requirements. As shown in the figure, the case without delay requirement has an extreme delay variance. However, if setting the delay requirement  $D_{req} = 0.1$  (s), the delay variance can be also improved to about  $10^{-3}$ . For  $D_{req} = 0.01$  (s), the delay variance can be controlled to about  $10^{-4}$ .

In the above figures, we investigate the interactions among the delay, capacity, and coverage. It is shown that optimal cell capacity and coverage can be achieved simultaneously, and QoS (delay and jitter) can be provided at the expense of lower cell capacity and coverage.

### B. Effect of Ring Sectorization

Fig. 12 compares the effect of ring sectorization on the cell capacity. As shown in the figure, when both rings  $A_1$  and  $A_2$  are sectorized, the optimal number of rings increases to  $n = 4$ . Moreover, one can observe that if sectorizing ring  $A_1$ , the optimal cell throughput can be improved by 35% over the case without sectorization. If both rings  $A_1$  and  $A_2$  are sectorized, the optimal cell throughput can be further improved by 37% over the case with only sectorizing  $A_1$ .

Obviously, the more the rings are divided into sectors, the better the cell capacity. For sectorizing more rings, however, a more sophisticated frequency planning is needed to allocate more available channels to each mesh cell.

## VIII. CONCLUSION AND FUTURE WORKS

In this paper, we have investigated a scalable multichannel ring-based WMN with QoS support. Subject to the QoS requirement, an optimization approach is proposed to maximize the cell capacity and coverage for the considered WMN.

From the system architecture perspective, the proposed WMN has two key elements. First, a simple ring-based frequency planning has been employed to improve the capacity

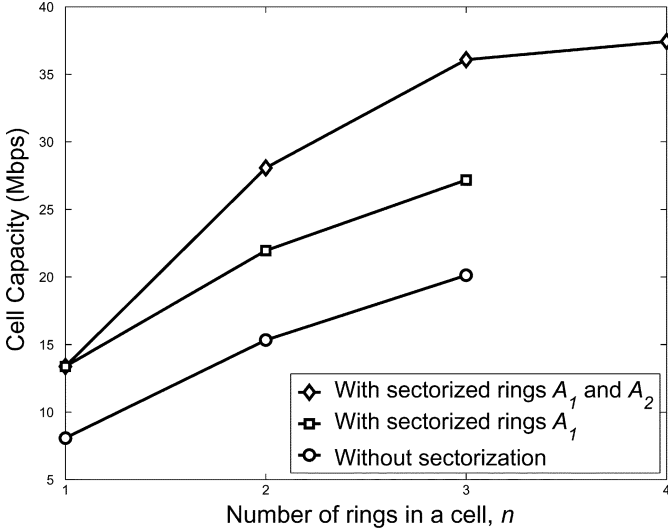


Fig. 12. Effect of ring sectorization on the cell throughput, for the delay requirement  $D_{\text{req}} = 0.01$  (s).

with QoS support, and to make the system more scalable in terms of coverage. Second, sectoring the congested inner rings has been suggested to resolve the bottleneck issue of the WMNs.

From the system design perspective, this paper has other three important components. First, we have proposed a PHY/MAC cross-layer analytical model to evaluate the throughput of the proposed WMN. Second, we have developed a queueing model to analyze the delay and jitter. Third, we have applied the MINLP optimization approach to determine the optimal number of rings in a mesh cell and the associated ring widths in the proposed ring-based WMN. Numerical results have shown that the optimal system parameters (i.e., the number of rings and ring widths) can be determined analytically, and the goals of capacity enhancement and QoS support can be fulfilled at a slight cost of coverage performance.

Many interesting issues are worthwhile for further investigation from this work. First, besides the bottleneck issue near the central gateway, the WMNs also need to resolve the energy fairness issue. In WMNs, most traffic is delivered either to or from the central gateway [2]. The users near the central gateway have to spend more energy to relay traffic than the other users, which leads to energy unfairness. Even worse, if the users near the central gateway rapidly exhaust their batteries, the mesh network will not function normally. Therefore, how to achieve energy fairness for WMNs is an important issue in the future.

Second, the impact of power control needs to be further investigated. Although higher transmit power can increase the maximum allowable hop distance and the data rate in relay link, it also increases contention collisions and lowers the efficiency of spatial frequency reuse. Hence, how to determine the proper transmit power to achieve the best tradeoff among energy efficiency, QoS, capacity, and coverage in a ring-based WMN is an essential task. In addition, there are some other interesting topics, including how to support differentiated services with different priorities, how to design the enhanced multichannel MAC protocol for WMN, and to evaluate the impacts of cooperative communications on the ring-based WMN.

## APPENDIX

### SUCCESSFUL PROBABILITIES, $s_{1,j}$ AND $s_{2,j}$

Now, we derive the probabilities  $s_{1,j}$  and  $s_{2,j}$  mentioned in Section IV-C. In Fig. 6, suppose that the considered area of angle  $2\theta_{S,i}$  is influenced by two neighboring transmitters. Let  $\omega$  represent the position of the contending user  $P'$ ,  $\psi_L$  and  $\psi_R$  be the positions of the neighboring transmitters  $P_L$  and  $P_R$ . Accordingly, the central angles for regions  $\{A_{S,i} - Y_L\}$  and  $\{A_{S,i} - Y_R\}$  can be written as  $\alpha_L = \theta_{S,i} - \max(0, \psi_L + \theta_{S,i} - \theta_{W,i})$  and  $\alpha_R = \theta_{S,i} - \max(0, \psi_R + \theta_{S,i} - \theta_{W,i})$ , respectively. Suppose that  $\tau_e = \tau(1 - P_0)$  is the effective transmission probability for one user. Then, given the positions  $\omega$ ,  $\psi_L$ , and  $\psi_R$ , the conditional probability that the left-side mutually interfered region of user  $P$  contains a successful transmission can be expressed as

$$s_{1,j}(\psi_L, \psi_R, \omega) = \begin{cases} \left( \frac{\frac{\rho a_i}{2\pi} \alpha_L - 1}{1} \right) \tau_e (1 - \tau_e)^{\frac{\rho a_i}{2\pi} (\beta_L + \beta'_L) - 2}, & \text{for } \max(0, \psi_R - \theta_{S,i}) \leq \omega \leq \max(0, \theta_{S,i} - \psi_L) \\ 0, & \text{otherwise.} \end{cases} \quad (48)$$

In (48), the term  $\left( \frac{\rho a_i / 2\pi \alpha_L - 1}{1} \right)$  represents the probability that only user  $P'$  sends an RTS request in the left-side mutually interfered region of user  $P$ . The term  $(1 - \tau_e)^{\frac{\rho a_i}{2\pi} (\beta_L + \beta'_L) - 2}$  accounts for the probability that all the users except for  $P$  and  $P'$  in the adjacent wireless collision domains of  $P'$  are in backoff or idle, where  $\beta_L = \min(\omega + \theta_{W,i}, (\theta_{S,i} + \theta_{W,i}) - (\psi_L + \theta_{S,i})) = \min(\omega + \theta_{W,i}, \theta_{W,i} - \psi_L)$  and in the same way  $\beta'_L = \min(\theta_{W,i} - \omega, \theta_{W,i} - \psi_R)$ . In addition, the condition for  $\omega$  means that both the neighboring transmitters  $P_L$  and  $P_R$  are not inside the working-in-vain regions of  $P'$ .

By the same method, the conditional probability that each mutually interfered region of user  $P$  contains a successful transmission can be obtained from

$$s_{2,j}(\psi_L, \psi_R, \omega) = s_{1,j}(\psi_L, \psi_R, \omega) \left[ \left( \frac{\frac{\rho a_i}{2\pi} \beta_R}{1} \right) \tau_e (1 - \tau_e)^{\frac{\rho a_i}{2\pi} \beta'_R - 1} \right]. \quad (49)$$

Here, the term within brackets represents the probability that the right-side mutually interfered region of user  $P$  also contains a successful transmission, where  $\beta_R = \max(0, (\theta_{S,i} + \theta_{W,i}) - (\psi_R + \theta_{S,i} - 1) - (\theta_{W,i} - \omega)) = \max(0, (\theta_{S,i} - \psi_R) - (\theta_{W,i} - \omega))$  and  $\beta'_R = \max(0, (\theta_{S,i} + \theta_{W,i}) - (\psi_R + \theta_{S,i}) - (\theta_{W,i} - \omega)) = \max(0, \omega - \psi_R)$ .

By averaging over the positions  $\omega$ ,  $\psi_L$ , and  $\psi_R$ , the probabilities  $s_{1,j}$  and  $s_{2,j}$  for  $j = 2$  can be computed by

$$s_{t,j} = \frac{1}{\theta_{W,i}^2} \int_0^{\theta_{W,i}} \int_0^{\theta_{W,i}} \int_0^{\alpha_L} \frac{s_{t,j}(\psi_L, \psi_R, \omega)}{\alpha_L} d\omega d\psi_R d\psi_L, \quad \text{for } t = 1, 2. \quad (50)$$

In this section, we take the case of  $j = 2$  as an example to evaluate the successful probability  $s_{t,j}$ . By the same reasoning, one can also calculate the probabilities  $s_{t,j}$  for  $j = 0, 1$ . Thus, the detailed derivations are omitted here.

## REFERENCES

- [1] R. Pabst, "Relay-based deployment concepts for wireless and mobile broadband radio," *IEEE Commun. Mag.*, vol. 42, no. 9, pp. 80–89, Sep. 2004.
- [2] J. Jun and M. Sichertu, "The nominal capacity of wireless mesh networks," *IEEE Wireless Commun. Mag.*, vol. 10, no. 5, pp. 8–14, Oct. 2003.
- [3] I. Akyildiz, X. Wang, and W. Wang, "Wireless mesh networks: A survey," *Comput. Netw.*, vol. 47, pp. 445–487, Mar. 2005.
- [4] *MeshDynamics Website*, [Online]. Available: <http://www.meshdynamics.com>
- [5] K. Jain, "Impact of interference on multi-hop wireless network performance," in *Proc. ACM MobiCom*, Sept. 2003, pp. 66–80.
- [6] S. Naghian and J. Tervonen, "Semi-infrastructure mobile ad-hoc mesh networking," in *Proc. IEEE PIMRC*, Sep. 2003, pp. 1069–1073.
- [7] P. Gupta and P. R. Kumar, "The capacity of wireless networks," *IEEE Trans. Inf. Theory*, vol. 46, pp. 388–404, Mar. 2000.
- [8] J. Li, "Capacity of ad hoc wireless networks," in *Proc. ACM MobiCom*, July 2001, pp. 61–69.
- [9] A. E. Gammal, J. Mammen, B. Prabhakar, and D. Shah, "Throughput-delay trade-off in wireless networks," in *Proc. IEEE INFOCOM*, Mar. 2004, pp. 464–475.
- [10] E. Perivalov and R. S. Blum, "Delay-limited throughput of ad hoc networks," *IEEE Trans. Commun.*, vol. 52, no. 11, pp. 1957–1968, Nov. 2004.
- [11] M. J. Neely and E. Modiano, "Capacity and delay tradeoffs for ad-hoc mobile networks," *IEEE Trans. Inf. Theory*, vol. 51, no. 6, pp. 1917–1937, Jun. 2005.
- [12] J.-H. Huang, L.-C. Wang, and C.-J. Chang, "Coverage and capacity of a wireless mesh network," in *Proc. WirelessCom*, Jun. 2005, pp. 458–463.
- [13] G. Bianchi, "Performance analysis of the IEEE 802.11 distributed coordination function," *IEEE J. Sel. Areas Commun.*, vol. 18, no. 3, pp. 535–547, Mar. 2000.
- [14] P. Chatzimisios, A. C. Boucouvalas, and V. Vitsas, "Packet delay analysis of the IEEE MAC 802.11 protocol," *Inst. Elect. Eng. Electron. Lett.*, vol. 39, pp. 1358–1359, Sep. 2003.
- [15] X. J. Dong and P. Variya, "Saturation throughput analysis of IEEE 802.11 wireless LANs for a lossy channel," *IEEE Commun. Lett.*, vol. 9, no. 2, pp. 100–102, Feb. 2005.
- [16] H. A. Willebrand and B. S. Ghuman, "Fiber optics without fiber," *IEEE Spectr.*, vol. 38, pp. 40–45, Aug. 2001.
- [17] *Wireless LAN Medium Access Control (MAC) and Physical Layer (PHY) Specifications*, IEEE 802.11, Aug. 1998, IEEE Standard.
- [18] *Part 11: Wireless LAN, Medium Access Control (MAC) and Physical Layer (PHY) Specifications: High-Speed Physical Layer in the 5 GHz Band*, IEEE 802.11a, Supplement to IEEE 802.11 Standard, Sept. 1999.
- [19] Y. C. Yang and K. C. Chua, "A capacity analysis for the IEEE 802.11 MAC protocol," *Wireless Netw.*, pp. 159–171, July 2001.
- [20] L. J. Cimini JR., "Packet shaping for mixed rate 802.11 wireless networks," U.S. Patent 0030133427, Jul. 2003.
- [21] M. Heusse, "Performance anomaly of 802.11b," in *Proc. IEEE INFOCOM*, Mar. 2003, pp. 836–843.
- [22] D. Gross and C. M. Harris, *Fundamentals of Queueing Theory*, 3rd ed. New York: Wiley, 1998.
- [23] *Cisco Aironet 1200 Series Access Point*, [Online]. Available: <http://www.cisco.com/en/US/products/hw/wireless/ps430/index.htm>, CISCO



**Jane-Hwa Huang** received the B.S., M.S., and Ph.D. degrees in electrical engineering from the National Cheng-Kung University, Tainan, Taiwan, R.O.C., in 1994, 1996, and 2003, respectively.

He joined the Department of Communication Engineering, National Chiao-Tung University (NCTU), Hsinchu, Taiwan, as a Postdoctoral Researcher from 2004 to January 2006, and a Research Assistant Professor since January 2006. His current research interests are in the areas of wireless networks, wireless multihop communications, and radio resource

management.



**Li-Chun Wang** (S'92–M'96–SM'06) received the B.S. degree from the National Chiao-Tung University (NCTU), Hsinchu, Taiwan, R.O.C., the M.S. degree from the National Taiwan University, Taipei, Taiwan, and the M.Sci. and Ph.D. degrees from the Georgia Institute of Technology, Atlanta, in 1986, 1988, 1995, and 1996, respectively, all in electrical engineering.

From 1990 to 1992, he was with the Telecommunications Laboratories of the Ministry of Transportation and Communications, Taiwan (currently, the Telecom Laboratories of Chunghwa Telecom Company). In 1995, he was affiliated with Bell Northern Research, Northern Telecom, Inc., Richardson, TX. From 1996 to 2000, he was with AT&T Laboratories, where he was a Senior Technical Staff Member in the Wireless Communications Research Department. Since August 2000, he has been an Associate Professor with the Department of Communication Engineering, National Chiao-Tung University. He is the holder of a U.S. patent with three more pending. His current research interests are in the areas of cellular architectures, radio network resource management, cross-layer optimization, and cooperation wireless communications networks.

Dr. Wang was a corecipient (with G. L. Stuer and C.-T. Lea) of the 1997 IEEE Jack Neubauer Best Paper Award for his paper "Architecture Design, Frequency Planning, and Performance Analysis for a Microcell/Macrocell Overlaying System," which appeared in the IEEE TRANSACTIONS ON VEHICULAR TECHNOLOGY (best systems paper published in 1997 by the IEEE Vehicular Technology Society). He is currently an Associate Editor for the IEEE TRANSACTIONS ON WIRELESS COMMUNICATIONS.



**Chung-Ju Chang** (S'81–M'85–SM'94–F'05) was born in Taiwan, R.O.C., in August 1950. He received the B.E. and M.E. degrees in electronics engineering from National Chiao-Tung University (NCTU), Hsinchu, Taiwan, in 1972 and 1976, respectively, and the Ph.D. degree in electrical engineering from National Taiwan University (NTU), Taipei, Taiwan, in 1985.

From 1976 to 1988, he was with Telecommunication Laboratories, Directorate General of Telecommunications, Ministry of Communications, Taiwan, as a Design Engineer, Supervisor, Project Manager, and then Division Director. There, he was involved in designing digital switching system, RAX trunk tester, ISDN user-network interface, and ISDN service and technology trials in Science-Based Industrial Park. In the meantime, he also acted as a Science and Technical Advisor for the Minister of the Ministry of Communications from 1987 to 1989. In 1988, he joined the Faculty of the Department of Communication Engineering and the Center for Telecommunications Research, College of Electrical Engineering and Computer Science, NCTU, as an Associate Professor. He has been a Professor since 1993. He was Director of the Institute of Communication Engineering from August 1993 to July 1995, Chairman of Department of Communication Engineering from August 1999 to July 2001, and the Dean of the Research and Development Office from August 2002 to July 2004. Also, he was an Advisor for the Ministry of Education to promote the education of communication science and technologies for colleges and universities in Taiwan during 1995–1999; he is acting as a Committee Member of the Telecommunication Deliberate Body, Taiwan. His research interests include performance evaluation, wireless communication networks, and broadband networks.

Dr. Chang is a member of the Chinese Institute of Engineers (CIE). He serves as Editor for the *IEEE Communications Magazine* and Associate Editor for IEEE TRANSACTIONS ON VEHICULAR TECHNOLOGY.